818. Free flexural vibrations of a piezoelectric bimorph plate with periodic edge conditions

Pilkee Kim[1], Jeehyun Jung[2], Jongwon Seok[3]
Chung-Ang University, Seoul, Republic of Korea
E-mail: [1]*pilgu09@hotmail.com*, [2]*jisign29@naver.com*, [3]*seokj@cau.ac.kr*

(Received 12 July 2012; accepted 4 September 2012)

Abstract. This work analyzes the vibrations of a fully-electroded annular piezoelectric bimorph plate with a free inner edge and an outer edge that is built-in with a periodicity. To this end, a variational formulation with the extensive use of Lagrange multipliers for a bimorph plate with polar orthorhombic symmetry is performed first. The mechanical displacement and the electric potential that must satisfy constraint conditions at the electrodes are expanded as the sums of powers in the thickness coordinate. The resulting piezoelectric bimorph plate equations are used along with the introduction of appropriate Lagrange multipliers to analyze the polar orthorhombic annular sectorial plates with free radial and inner circumferential edges, and an entirely built-in or free outer edge. The results are then combined to obtain the solutions for the mixed boundary value problem. The extended Hamilton's principle with the method of Lagrange multipliers is employed, followed by a Frobenius-type series expansion for solution functions. The eigensolutions are calculated from the resulting transcendental equation and compared with those obtained from an FEA to ensure the validity of the procedure.

Keywords: polar orthorhombic bimorph, annular plate, mixed boundary condition with periodicity, variational approximation procedure, Lagrange multipliers method.

Introduction

The vibration problem of annular and circular plates has been researched extensively using various theoretical or numerical approaches due to their wide range of applications in sensors and actuators. The free vibrations of annular and circular plates with various boundary conditions were well summarized by Leissa [1]. Free vibration problems of isotropic annular sector plates with simply supported radial edges were solved earlier using an exact method applied to a thin plate model [2]. Kobayashi et al. [3] obtained an analytical solution for the vibration of a Mindlin annular sector plate [4] with two simply supported radial edges and two free circumferential edges. Additionally, several numerical and semi- analytical studies have been performed to obtain approximate solutions for annular plates with various boundary conditions [5-16] by using the Rayleigh-Ritz method [5, 10], the Frobenius method [6], the finite difference method [7], the strip distribution transfer function method [11], the mode subtraction method [12], finite element method [13, 15], and so on. However, to the best of the authors' knowledge, variational treatment of the vibration problem of annular piezoelectric plates with mixed boundary conditions has not been reported.

This study analyzes the flexural vibrations of an annular polar orthorhombic bimorph plate with a mixed edge condition by means of variational approximation treatment [17-19]. The annular plate with a mixed outer circumferential edge with periodicity can be pictured as a combination of two types of sectorial plates with free inner edges, and one with a built-in outer edge and the other with a free outer edge. This problem applies to a bounded region containing several separated volumes with internal surfaces of discontinuity. Therefore, we must determine the dispersion relationships for both cases separately. These analyses are performed by employing the extended Hamilton principle with the Lagrange multipliers method within the framework of 2-D plate theory. The method of separation of variables is used, and the solution functions satisfying the differential equation in the radial direction are obtained by introducing a Frobenius-type series expansion [20, 21] about a regular point. The dispersion relationships are

obtained by making the solution functions satisfy exactly the edge conditions on the two facing circumferential edges. For the remaining portion of the variational equation, in which all edge conditions occur as natural type, only the waves satisfying the dispersion relationships are employed as solution functions to obtain the eigensolutions. The dispersion relationships obtained in the foregoing problems are then combined using the Lagrange multipliers formalism to obtain eigensolutions for the annular polar orthorhombic plate with a mixed boundary condition.

Mathematical modeling

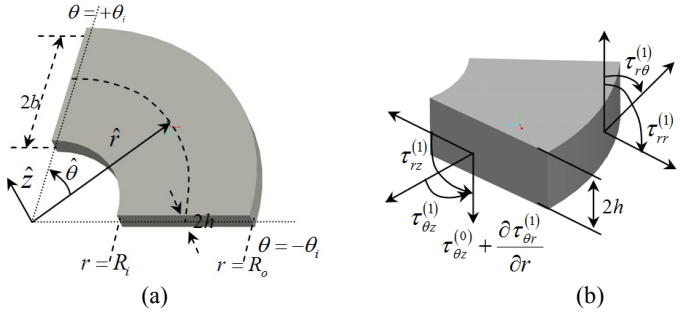

(a) (b)

Fig. 1. (a) 3-D view of an annular sector plate and
(b) a plane view of an element with stress resultants and coordinates

Consider an annular sector plate with faces of area S at $x_3 = \pm h$ in a fixed cylindrical co-ordinate system ($\hat{r}$, $\hat{\theta}$, $\hat{z}$) shown in Fig. 1(a). The x_1 and x_2 are the coordinates attached to the middle plane of the plate. The inner and outer radii are R_i and R_o, respectively, and the potential difference between the top and middle electrodes (and also the bottom and middle ones) is denoted as V_e. Fig. 1(b) shows an element of the annular sector plate with the relevant stress resultants required in the description of flexure of the plate. Introducing the modified Hamilton's principle of linear piezoelectricity [17], the coupled variational equation for a bounded body containing an internal surface of discontinuity can be represented by:

$$\delta\int_{t_0}^{t} dt\sum_{m=1}^{2}\Big[\int_{V^{(m)}}\Big[(1/2)\rho^{(m)}\dot{u}_j^{(m)}\dot{u}_j^{(m)} - H^{(m)}(S_{kl}^{(m)}, E_k^{(m)})\Big]dV + \int_{S_N^{(m)}}\Big(\overline{t}_k^{(m)}u_k^{(m)} - \overline{\sigma}^{(m)}\varphi^{(m)}\Big)dS$$
$$+\int_{S_C^{(m)}}\lambda_k^{(m)}(u_k^{(m)} - \overline{u}_k^{(m)})dS - \int_{S_C^{(m)}} l^{(m)}(\varphi^{(m)} - \overline{\varphi}^{(m)})dS\Big]$$
$$+\delta\int_{t_0}^{t} dt\int_{S^{(d)}}\lambda_k^{(d)}(u_k^{(2)} - u_k^{(1)})dS - \delta\int_{t_0}^{t} dt\int_{S^{(d)}} l^{(d)}(\varphi^{(2)} - \varphi^{(1)})dS = 0, \quad (1)$$

where t, δ, $\rho^{(m)}$, $H^{(m)}$, $s_{kl}^{(m)}$, and $E_k^{(m)}$ indicate the time, the variational operator, the mass density, the Hamiltonian, the strain tensor, and the electric field (of the m^{th} volume), respectively; $S_N^{(m)}$, $S_C^{(m)}$, and $S^{(d)}$ indicate the portion of the m^{th} surface on which the traction $t_k^{(m)}$ and/or the charge $\sigma^{(m)}$ are prescribed, the portion of the m^{th} surface on which the mechanical displacement $u_k^{(m)}$ and/or the electrical potential $\varphi^{(m)}$ are prescribed, and the surface of discontinuity, respectively; and $\lambda_k^{(m)}$, $l^{(m)}$, $\lambda_k^{(d)}$, and $l^{(d)}$ are the Lagrange multipliers. In Eq. (1), a bar over a symbol signifies the prescribed quantity.

This work assumes that the system obeys the linear constitutive equations, the infinitesimal strain-displacement relations, and the quasi-static electric field-electric potential relations [17]. Note that the actual coupling between the mechanical and electrical quantities in Eq. (1) occurs in the constitutive equations of the piezoelectricity and, under the thin plate assumptions

employed here, the electrical part is reflected in the constitutive equations for the mechanical part.

The 2-D variational equations for thin plates under all conditions (both natural and constraint types) arising as natural conditions can be obtained from the appropriate 3-D equations [17]. Using a series-expansion method and introducing the cylindrical coordinate system, we can obtain the following 2-D variational equation for the flexural portion of an annular plate with a free inner circumferential edge, a built-in or free outer edge, and two free radial edges:

$$\int_A dS\Big[\Big\{\tau_{rz,r}^{(0)}+(\tau_{\theta z,\theta}^{(0)}+\tau_{rz}^{(0)})/r-2\rho h\ddot{w}\Big\}\delta w+\Big\{\tau_{rr,r}^{(1)}+\tau_{\theta z,\theta}^{(0)}/r+(\tau_{rr}^{(1)}-\tau_{\theta\theta}^{(1)})/r-\tau_{rz}^{(0)}\Big\}\delta u_r^{(1)}$$
$$+\Big\{\tau_{r\theta,r}^{(1)}+(\tau_{\theta\theta,\theta}^{(1)}+2\tau_{r\theta}^{(1)})/r-\tau_{\theta z}^{(0)}\Big\}\delta u_\theta^{(1)}\Big]-\int_{R_i}^{R_o}dr\Big[(\tau_{\theta z}^{(0)}+\tau_{\theta r,r}^{(1)})\delta w-\tau_{\theta\theta}^{(1)}/r\delta w_{,\theta}\Big]_{-\Theta}^{\Theta}$$
$$-\int_{-\Theta}^{\Theta}rd\theta\Big[(\tau_{rz}^{(0)}+\tau_{r\theta,\theta}^{(1)}/r)\delta w-\tau_{rr}^{(1)}\delta w_{,r}\Big]_{r=R_i}-\Big[\int_{R_i}^{R_o}dr\Big\{(\tau_{\theta z}^{(0)}+\tau_{\theta r,r}^{(1)})\delta w-\tau_{\theta\theta}^{(1)}/r\delta w_{,\theta}\Big\}\Big]_{\theta=-\Theta}^{\theta=\Theta}$$
$$+2\Big[\tau_{\theta r}^{(1)}\delta w\Big]_{r=R_i,\theta=-\Theta}^{r=R_i,\theta=\Theta}+\Phi=0, \tag{2}$$

where the time integration has been omitted and Φ is given, for a free and built-in outer edges, respectively, as:

$$\Phi=\int_{-\Theta}^{\Theta}rd\theta\Big[\Big(\tau_{rz}^{(0)}+\tau_{r\theta,\theta}^{(1)}/r\Big)\delta w-\tau_{rr}^{(1)}\delta w_{,r}\Big]_{r=R_o}-2\Big[\tau_{\theta r}^{(1)}\delta w\Big]_{r=R_o,\theta=-\Theta}^{r=R_o,\theta=\Theta}\quad\text{and} \tag{3a}$$

$$\Phi=-\int_{-\Theta}^{\Theta}rd\theta\Big[w\delta\Big(\tau_{rz}^{(0)}+\tau_{r\theta,\theta}^{(1)}/r\Big)-w_{,r}\delta\tau_{rr}^{(1)}\Big]_{r=R_o}+\Big[w\delta\tau_{\theta r}^{(1)}-\tau_{\theta r}^{(1)}\delta w\Big]_{r=R_o,\theta=-\Theta}^{r=R_o,\theta=\Theta}, \tag{3b}$$

and

$$u_j=\sum_{n=0}^{N}[x_3^n u_i^{(n)}(x_a,t)],\quad N=1\ \text{for}\ i=1,2\ \text{and}\ N=2\ \text{for}\ i=3,$$
$$\tau_{ij}^{(n)}=\tau_{ij}^{(1,n)}+\tau_{ij}^{(2,n)},\quad \tau_{ij}^{(1,n)}=\int_0^h\tau_{ij}x_3^n dx_3,\quad \tau_{ij}^{(2,n)}=\int_{-h}^0\tau_{ij}x_3^n dx_3,\quad n=1,2,$$
$$\big[f(x)\big]_{x=a}^{x=b}=f(b)-f(a),\quad \big[g(x)\big]_{x=c}=g(c),\ w=u_z^{(0)}. \tag{4}$$

Since the wavelength along the thin plates in elementary flexure is much larger than the thickness, the constitutive equations for $\tau_{rz}^{(0)}$ and $\tau_\theta^{(0)}$ may be ignored. Using the 2-D strain-displacement relations [19], the 2-D constitutive equations for the flexure of the piezoelectric plate with polar orthorhombic symmetry can be readily obtained (details are not provided here due to space limitation).

Since the differential equation obtained from Eq. (2) is singular at $r = 0$, an expansion about a regular point ($r = r_0$) is introduced and yields four independent series solutions, which converge quickly in the region of interest [21]. The resulting differential equation can be obtained in the form:

$$r^2\tau_{rr,rr}^{(1)}+2r\tau_{r\theta,r\theta}^{(1)}+\tau_{\theta\theta,\theta\theta}^{(1)}+2\tau_{r\theta,\theta}^{(1)}+2r\tau_{rr,r}^{(1)}-r\tau_{\theta\theta,r}^{(1)}=2\rho hr^2\ddot{w}. \tag{5}$$

The four conditions prescribed to the inner and outer edges are:

$$[\tau_{rr}^{(1)}]_{r=R_i}=0,\quad [\tau_{rz}^{(0)}+\tau_{r\theta,\theta}^{(1)}/r]_{r=R_i}=0, \tag{6a}$$

$$\begin{cases}[\tau_{rr}^{(1)}]_{r=R_o}=0,\ [\tau_{rz}^{(0)}+\tau_{r\theta,\theta}^{(1)}/r]_{r=R_o}=0 & \text{for a free outer edge,}\\ [w]_{r=R_o}=0,\quad [w_{,r}]_{r=R_o}=0 & \text{for a built-in outer edge.}\end{cases} \tag{6b}$$

Using the separation of variables, the solution may take the form:

$$w(r,\theta,t) = \mathrm{Re}[\tilde{w}(r)e^{\mathrm{i}(\omega t-\xi\theta)}], \tag{7}$$

where Re[ ] means the real portion of the argument and will be dropped hereafter. Furthermore, for the purpose of generality, the following dimensionless quantities are introduced:

$$\bar{r} = \pi r/(2b),\ \bar{r}_0 = \pi r_0/(2b),\ \tilde{r} = \bar{r} - \bar{r}_0,\ \bar{\omega} = \pi/(2b)\sqrt{c_{66}/\rho},$$
$$\bar{\kappa} = \hat{\kappa}\bar{\omega}(2b/\pi)^2,\ \bar{\Omega} = \omega/\bar{\omega},\ T = (2c_{66}/c_{11}^*) + \hat{\nu},\ R = c_{22}^*/c_{11}^*, \tag{8}$$

where the expressions for c_{11}^*, and c_{22}^* can be found in [22]. Introducing a Frobenius-type expansion [23] into $\tilde{w}$ in Eq. (7), we can let $\tilde{w}$ be:

$$G_\varsigma(\tilde{r};\bar{\Omega},\xi) = \sum_{l=0}^{L}\bar{\alpha}_l^{(\varsigma)}(\bar{\Omega},\xi)\tilde{r}^{\varsigma+l-1},\quad \varsigma = 1,\cdots,4, \tag{9}$$

$$\tilde{w}(\tilde{r}) = \tilde{w}_1(\tilde{r}) + \tilde{w}_2(\tilde{r}) = \sum_{\varsigma=1}^{4}[A_\varsigma^{(1)}(\bar{\Omega},\xi)G_\varsigma(\tilde{r};\bar{\Omega},\xi)] + \sum_{\varsigma=1}^{4}[A_\varsigma^{(2)}(\bar{\Omega},\bar{V}_e)G_\varsigma(\tilde{r};\bar{\Omega},\xi=0)], \tag{10}$$

where L is a sufficiently large number satisfying the conditions for the convergence of the four solutions within the region of interest and $\tilde{w}_1(\tilde{r})$ satisfies the homogeneous parts of the edge conditions in Eq. (6), and $\tilde{w}_2(\tilde{r})$ satisfies the inhomogeneous parts; i.e., for β = 1, 2, we have the following edge equations to be satisfied:

(i) For an inner circumferential edge:

$$\begin{aligned}&[(\tilde{r}+\bar{r}_0)^2\tilde{w}_\beta'' + \hat{\nu}\{(\tilde{r}+\bar{r}_0)\tilde{w}_\beta' - \xi^2\delta_{\beta1}\tilde{w}_\beta\}]_{\tilde{r}=-\pi/2} = \delta_{\beta2}[\bar{V}_e(\tilde{r}+\bar{r}_0)^2]_{\tilde{r}=-\pi/2},\\ &[(\tilde{r}+\bar{r}_0)\{(\tilde{r}+\bar{r}_0)^2\tilde{w}_\beta''' + (\tilde{r}+\bar{r}_0)\tilde{w}_\beta'' - R\tilde{w}_\beta'\} + \xi^2\delta_{\beta1}\{(2T+R-\hat{\nu})\tilde{w}_\beta - (2T-\hat{\nu})(\tilde{r}+\bar{r}_0)\tilde{w}_\beta'\}]_{\tilde{r}=-\pi/2} = 0,\end{aligned} \tag{11a}$$

(ii) For an outer circumferential edge:

$$\begin{aligned}&[(\tilde{r}+\bar{r}_0)^2\tilde{w}_\beta'' + \hat{\nu}\{(\tilde{r}+\bar{r}_0)\tilde{w}_\beta' - \xi^2\delta_{\beta1}\tilde{w}_\beta'\}]_{\tilde{r}=\pi/2} = \delta_{\beta2}[\bar{V}_e(\tilde{r}+\bar{r}_0)^2]_{\tilde{r}=\pi/2},\\ &[(\tilde{r}+\bar{r}_0)\{(\tilde{r}+\bar{r}_0)^2\tilde{w}_\beta''' + (\tilde{r}+\bar{r}_0)\tilde{w}_\beta'' - R\tilde{w}_\beta'\} + \xi^2\delta_{\beta1}\{(2T+R-\hat{\nu})\tilde{w}_\beta\\ &-(2T-\hat{\nu})(\tilde{r}+\bar{r}_0)\tilde{w}_\beta'\}]_{\tilde{r}=\pi/2} = \delta_{\beta2}(1-\eta)[\bar{V}_e(\tilde{r}+\bar{r}_0)^2]_{\tilde{r}=\pi/2} \quad \text{for a free outer edge},\\ &[\tilde{w}_\beta]_{\tilde{r}=\pi/2},\ [\tilde{w}_\beta']_{\tilde{r}=\pi/2} = 0 \qquad\qquad \text{for a built-in outer edge},\end{aligned} \tag{11b}$$

where δ_{ab} is the Kronecker delta function.

Under this circumstance, we can then obtain the four coupled homogeneous linear equations with only $A_\varsigma^{(1)}$. The conditions required to obtain nontrivial solutions for these equations are a vanishing determinant of the 4×4 matrix associated with the vector composed of $A_\varsigma^{(1)}$, which leads to the dispersion relationships and the associated amplitude ratios of $A_\varsigma^{(1)}$. Since the solution function in Eq. (10) satisfies the differential equation and the four circumferential edge conditions exactly, the remaining portion of the variational equation is for the two radial edges and four corners. The final form of the remaining variational equation can be written as:

$$\begin{aligned}\int_{-\pi/2}^{\pi/2} d\tilde{r}\Big[\Big[&Rw_{,\theta\theta\theta} - (2T-R)(\tilde{r}+\bar{r}_0)w_{,\theta}' + 2T(\tilde{r}+\bar{r}_0)^2 w_{,\theta}'' + 2Tw_{,\theta}\\ &-\hat{\nu}\{-2(\tilde{r}+\bar{r}_0)w_{,\theta}' + (\tilde{r}+\bar{r}_0)^2 w_{,\theta}'' + 2w_{,\theta}\}\Big]\delta w\\ &-\Big[\hat{\nu}(\tilde{r}+\bar{r}_0)^2 w'' + R\{w_{,\theta\theta} + (\tilde{r}+\bar{r}_0)w'\} - \bar{V}_e\eta(\tilde{r}+\bar{r}_0)^2\Big]\delta w_{,\theta}\Big]_{\theta=-\Theta}^{\theta=\Theta}\end{aligned}$$

$$+2(T-\hat{\nu})(\tilde{r}+\overline{r}_0)\left[\{(\tilde{r}+\overline{r}_0)w'_{,\theta}-w_{,\theta}\}\delta\tilde{w}\right]^{\tilde{r}=-\pi/2,\theta=\Theta}_{\tilde{r}=-\pi/2,\theta=-\Theta}+\Psi=0, \tag{12}$$

where Ψ is given, for free and built-in outer edges, respectively, as:

$$\Psi=-2(T-\hat{\nu})(\tilde{r}+\overline{r}_0)\left[\{(\tilde{r}+\overline{r}_0)w'_{,\theta}-w_{,\theta}\}\delta\tilde{w}\right]^{\tilde{r}=\pi/2,\theta=\Theta}_{\tilde{r}=\pi/2,\theta=-\Theta} \quad \text{and} \tag{13a}$$

$$\Psi=\begin{cases}-(T-\hat{\nu})(\tilde{r}+\overline{r}_0)\left[\{(\tilde{r}+\overline{r}_0)w'_{,\theta}-w_{,\theta}\}\delta\tilde{w}\right]^{\tilde{r}=\pi/2,\theta=\Theta}_{\tilde{r}=\pi/2,\theta=-\Theta}\\ +(T-\hat{\nu})(\tilde{r}+\overline{r}_0)\left[\tilde{w}\delta\{(\tilde{r}+\overline{r}_0)w'_{,\theta}-w_{,\theta}\}\right]^{\tilde{r}=\pi/2,\theta=\Theta}_{\tilde{r}=\pi/2,\theta=-\Theta}.\end{cases} \tag{13b}$$

When N dispersion curves are taken, the solution functions for both free and built-in inner edges can be represented using the suppressed index notation in the form:

$$w=\sum_{\varsigma=1}^{4}\left[\sum_{\mu=1}^{N}\sum_{\upsilon=1}^{2}B_{\mu\upsilon}\overline{A}^{(1)}_{\varsigma}G_{\varsigma}\sin(\xi^{(\mu)}\theta+(\upsilon-1)\pi/2)+\overline{A}^{(2)}_{\varsigma}G_{\varsigma}\right]e^{i\bar{\Omega}\tau}, \tag{14}$$

and we can obtain $2N$ homogeneous equations with $2N$ unknown constants $B_{\mu\upsilon}$ for the homogeneous case ($\overline{V}_e = 0$) because all $A^{(2)}_{\varsigma}$ vanish. The conditions required to have nontrivial solutions to these $2N$ coupled equations yield the eigenvalues and the associated amplitude ratios that result in mode shapes. For an inhomogeneous case, however, we can obtain $2N$ inhomogeneous equations with $2N$ unknown constants, $B_{\mu\upsilon}$, which can result in solutions to the forced vibration problem with a given non-vanishing $\overline{V}_e$.

Consider a thin fully-electroded annular piezoelectric bimorph plate with a free inner edge and an outer edge that is built-in with a periodicity. If the annular plate includes P edges of discontinuity, then the number of volumes that must be treated independently should be P, and the variational equation should be modified to include the associated continuity conditions. Let the outer circumferential edge be divisible into P sub-plates with a periodicity of $2\pi/P$ in angle, and let the outer circumferential edge of the first sector (counted counterclockwise from the origin of the global coordinate system) be built-in. In addition, let the solution function satisfying the differential equation and the edge conditions be:

$$w^{(\chi)}=\sum_{p=1}^{4}\left[\sum_{n=1}^{N^{(\chi)}}\sum_{q=1}^{2}\overset{(\chi)}{B}_{nq}\overset{(\chi)}{A}^{(1)}_{p}\overset{(\chi)}{G}_{p}\sin(\overset{(\chi)}{\xi}^{(n)}\theta+(q-1)\pi/2)+\overset{(\chi)}{A}^{(2)}_{p}\overset{(\chi)}{G}_{p}\right]e^{i\bar{\Omega}\tau}, \tag{15}$$

where the superscript (χ) means quantity associated with the χ th sectorial plate, $\chi = 2j–1$ for the free inner and built-in outer circumferential edge conditions, $\chi = 2j$ for the free inner and free outer circumferential edge conditions, and $j = 1, \ldots, P/2$. Since the solution functions, Eq. (15), satisfy all the portions of the variational equation except those of the radial edge and the corner conditions, all that remains in the variational equation is:

$$\begin{aligned}\sum_{i=1}^{P}\Bigg[\int_{-\pi/2}^{\pi/2}d\tilde{r}\Bigg[\Big[&Rw^{(i)}_{,\theta\theta\theta}-(2T-R)(\tilde{r}+\overline{r}_0)w^{(i)\prime}_{,\theta}+2T(\tilde{r}+\overline{r}_0)^2w^{(i)\prime\prime}_{,\theta}+2Tw^{(i)}_{,\theta}\\ &-\hat{\nu}\left\{-2(\tilde{r}+\overline{r}_0)w^{(i)\prime}_{,\theta}+(\tilde{r}+\overline{r}_0)^2w^{(i)\prime\prime}_{,\theta}+2w^{(i)}_{,\theta}\right\}\Big]\delta\tilde{w}^{(i)}\\ &-\left[\hat{\nu}(\tilde{r}+\overline{r}_0)^2w^{(i)\prime\prime}+R\left\{w^{(i)}_{,\theta\theta}+(\tilde{r}+\overline{r}_0)w^{(i)\prime}\right\}-\overline{V}_e\eta(\tilde{r}+\overline{r}_0)^2\right]\delta w^{(i)}_{,\theta}\Bigg]^{\theta=\Theta_i}_{\theta=-\Theta_i}\end{aligned}$$

$$
\begin{aligned}
&+2\left(T-\hat{\nu}^{*}\right)\left(\tilde{r}+\overline{r}_{0}\right)\left[\left\{\left(\tilde{r}+\overline{r}_{0}\right)w_{,\theta}^{(i)\prime}-w_{,\theta}^{(i)}\right\}\delta w^{(i)}\right]_{\tilde{r}=-\pi/2,\theta=-\Theta_i}^{\tilde{r}=-\pi/2,\theta=\Theta_i}\\
&-\left(T-\hat{\nu}^{*}\right)\left(\tilde{r}+\overline{r}_{0}\right)\left[\left\{\left(\tilde{r}+\overline{r}_{0}\right)w_{,\theta}^{(i)\prime}-w_{,\theta}^{(i)}\right\}\delta w^{(i)}\right]_{\tilde{r}=\pi/2,\theta=-\Theta_i}^{\tilde{r}=\pi/2,\theta=\Theta_i}\Bigg]\\
&+\sum_{j=1}^{P/2}\Bigg[\left(T-\hat{\nu}^{*}\right)\left(\tilde{r}+\overline{r}_{0}\right)\left[w^{(2j-1)}\delta\left\{\left(\tilde{r}+\overline{r}_{0}\right)w_{,\theta}^{(2j-1)\prime}-w_{,\theta}^{(2j-1)}\right\}\right]_{\tilde{r}=\pi/2,\theta=-\Theta_{2j-1}}^{\tilde{r}=\pi/2,\theta=\Theta_{2j-1}}\\
&-\left(T-\hat{\nu}^{*}\right)\left(\tilde{r}+\overline{r}_{0}\right)\left[\left\{\left(\tilde{r}+\overline{r}_{0}\right)w_{,\theta}^{(2j)\prime}-w_{,\theta}^{(2j)}\right\}\delta w^{(2j)}\right]_{\tilde{r}=\pi/2,\theta=-\Theta_{2j}}^{\tilde{r}=\pi/2,\theta=\Theta_{2j}}\\
&+\delta\int_{-\pi/2}^{\pi/2}d\tilde{r}\Bigg[\lambda_{V1}^{(j)}\left\{\left[w^{(2j-1)}\right]_{\theta=\Theta_{2j-1}}-\left[w^{(2j)}\right]_{\theta=-\Theta_{2j}}\right\}+\lambda_{V2}^{(j)}\left\{\left[w^{(2j-1)}\right]_{\theta=-\Theta_{2j-1}}-\left[w^{(\Delta\{2(j-1)\})}\right]_{\theta=\Theta_{\Delta\{2(j-1)\}}}\right\}\\
&+\lambda_{M1}^{(j)}\left\{\left[w_{,\theta}^{(2j-1)}\right]_{\theta=\Theta_{2j-1}}-\left[w_{,\theta}^{(2j)}\right]_{\theta=-\Theta_{2j}}\right\}+\lambda_{M2}^{(j)}\left\{\left[w_{,\theta}^{(2j-1)}\right]_{\theta=-\Theta_{2j-1}}-\left[w_{,\theta}^{(\Delta\{2(j-1)\})}\right]_{\theta=\Theta_{\Delta\{2(j-1)\}}}\right\}\\
&+\delta\Bigg\{\lambda_{C1+}^{(j)}\left[\left[w^{(2j-1)}\right]_{\theta=\Theta_{2j-1}}-\left[w^{(2j)}\right]_{\theta=-\Theta_{2j}}\right]_{\tilde{r}=\pi/2}+\lambda_{C2+}^{(j)}\left[\left[w^{(2j-1)}\right]_{\theta=-\Theta_{2j-1}}-\left[w^{(\Delta\{2(j-1)\})}\right]_{\theta=\Theta_{\Delta\{2(j-1)\}}}\right]_{\tilde{r}=\pi/2}\\
&+\lambda_{C1-}^{(j)}\left[\left[w^{(2j-1)}\right]_{\theta=\Theta_{2j-1}}-\left[w^{(2j)}\right]_{\theta=-\Theta_{2j}}\right]_{\tilde{r}=-\pi/2}+\lambda_{C2-}^{(j)}\left[\left[w^{(2j-1)}\right]_{\theta=-\Theta_{2j-1}}-\left[w^{(\Delta\{2(j-1)\})}\right]_{\theta=\Theta_{\Delta\{2(j-1)\}}}\right]_{\tilde{r}=-\pi/2}\Bigg\}\Bigg]\\
&=0,
\end{aligned}
\tag{16}
$$

where $\pm\Theta_i = (2i-1\pm1)\pi/P$ and $\Delta(k) = k$ (or P) for $k \neq 0$ (or $k = 0$).

Note that all the variations on the left-hand side of Eq. (16) are unconstrained everywhere except at t and t_0, where they are constrained as in the classical version of Hamilton's principle, and the Lagrange multipliers $\lambda_{Vi}^{(j)}$, $\lambda_{Mi}^{(j)}$, and $\lambda_{Ci\pm}^{(j)}$ (i = 1, 2) are varied freely. Therefore, the Lagrange multipliers can be obtained by taking the variations of the last eight terms in Eq. (16) and making the coefficient terms of all the independent variations vanish. Consequently, the most appropriate forms of the Lagrange multipliers can be obtained, after some straightforward calculations, in the form:

$$
\begin{aligned}
\lambda_{V1}^{(j)}=\frac{1}{2}\sum_{\chi=2j-1,2j}\Big[&-Rw_{,\theta\theta\theta}^{(\chi)}+\left(2T-R\right)\left(\tilde{r}+\overline{r}_{0}\right)w_{,\theta}^{(\chi)\prime}-2T\left(\left(\tilde{r}+\overline{r}_{0}\right)^{2}w_{,\theta}^{(\chi)\prime\prime}+w_{,\theta}^{(\chi)}\right)\\
&+\hat{\nu}\left(\left(\tilde{r}+\overline{r}_{0}\right)^{2}w_{,\theta}^{(\chi)\prime\prime}-2\left(\tilde{r}+\overline{r}_{0}\right)w_{,\theta}^{(\chi)\prime}+2w_{,\theta}^{(\chi)}\right)\Big]_{\theta=\hbar(\Theta_\chi)},
\end{aligned}
\tag{17a}
$$

$$
\begin{aligned}
\lambda_{V2}^{(j)}=\frac{1}{2}\sum_{\chi=\Delta\{2(j-1)\},\,2j-1}\Big[&-Rw_{,\theta\theta\theta}^{(\chi)}+\left(2T-R\right)\left(\tilde{r}+\overline{r}_{0}\right)w_{,\theta}^{(\chi)\prime}-2T\left(\left(\tilde{r}+\overline{r}_{0}\right)^{2}w_{,\theta}^{(\chi)\prime\prime}+w_{,\theta}^{(\chi)}\right)\\
&+\hat{\nu}\left(\left(\tilde{r}+\overline{r}_{0}\right)^{2}w_{,\theta}^{(\chi)\prime\prime}-2\left(\tilde{r}+\overline{r}_{0}\right)w_{,\theta}^{(\chi)\prime}+2w_{,\theta}^{(\chi)}\right)\Big]_{\theta=\lambda(\Theta_\chi)},
\end{aligned}
\tag{17b}
$$

$$
\lambda_{M1}^{(j)}=\frac{1}{2}\sum_{\chi=2j-1,\,2j}\left[\hat{\nu}\chi\left(\tilde{r}+\overline{r}_{0}\right)^{2}w^{(\chi)\prime\prime}+R\left(\tilde{r}+\overline{r}_{0}\right)w^{(\chi)\prime}+Rw_{,\theta\theta}^{(\chi)}-\overline{V}_{e}\eta\left(\tilde{r}+\overline{r}_{0}\right)^{2}\right]_{\theta=\hbar(\Theta_\chi)},
\tag{17c}
$$

$$
\lambda_{M2}^{(j)}=\frac{1}{2}\sum_{\chi=\Delta\{2(j-1)\},\,2j-1}\left[\hat{\nu}\left(\tilde{r}+\overline{r}_{0}\right)^{2}w^{(\chi)\prime\prime}+R\left(\tilde{r}+\overline{r}_{0}\right)w^{(\chi)\prime}+Rw_{,\theta\theta}^{(\chi)}-\overline{V}_{e}\eta\left(\tilde{r}+\overline{r}_{0}\right)^{2}\right]_{\theta=\lambda(\Theta_\chi)},
\tag{17d}
$$

$$
\lambda_{C1+}^{(j)}=\frac{1}{2}\sum_{\chi=2j-1,\,2j}\left[\left(T-\hat{\nu}\right)\left(\tilde{r}+\overline{r}_{0}\right)\left[\left(\tilde{r}+\overline{r}_{0}\right)w_{,\theta}^{(\chi)\prime}-w_{,\theta}^{(\chi)}\right]\right]_{\theta=\hbar(\Theta_\chi),\tilde{r}=+\pi/2},
\tag{17e}
$$

$$
\lambda_{C1-}^{(j)}=-\sum_{\chi=2j-1,\,2j}\left[\left(T-\hat{\nu}\right)\left(\tilde{r}+\overline{r}_{0}\right)\left[\left(\tilde{r}+\overline{r}_{0}\right)w_{,\theta}^{(\chi)\prime}-w_{,\theta}^{(\chi)}\right]\right]_{\theta=\hbar(\Theta_\chi),\tilde{r}=-\pi/2},
\tag{17f}
$$

$$\lambda_{C2+}^{(j)} = -\frac{1}{2}\sum_{\chi=\Delta\{2(j-1)\},\ 2j-1}\left[\left(T-\hat{\nu}^{*}\right)\left(\tilde{r}+\overline{r}_0\right)\left[\left(\tilde{r}+\overline{r}_0\right)w_{,\theta}^{(\chi)\prime}-w_{,\theta}^{(\chi)}\right]\right]_{\theta=\hbar(\Theta_\chi),\tilde{r}=+\pi/2}, \tag{17g}$$

$$\lambda_{C2-}^{(j)} = \sum_{\chi=\Delta\{2(j-1)\},\ 2j-1}\left[\left(T-\hat{\nu}^{*}\right)\left(\tilde{r}+\overline{r}_0\right)\left[\left(\tilde{r}+\overline{r}_0\right)w_{,\theta}^{(\chi)\prime}-w_{,\theta}^{(\chi)}\right]\right]_{\theta=\hbar(\Theta_\chi),\tilde{r}=-\pi/2}, \tag{17h}$$

where $\hbar(k)$ and $\hbar(k)$ are $+k$ (or $-k$) for odd (or even). It should be noted that since the Lagrange multipliers in Eq. (17) are arbitrary, the continuity conditions for the displacements and slopes are to be satisfied variationally.

Results and discussion

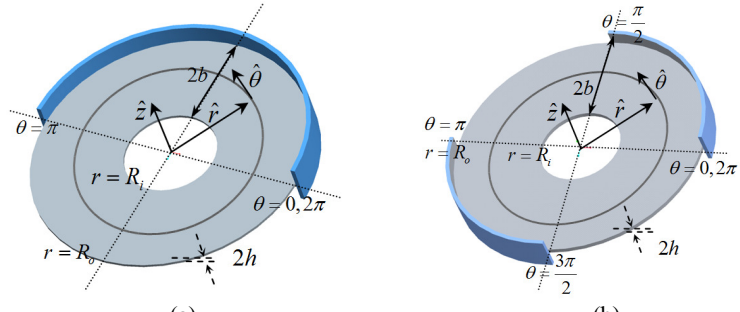

Fig. 2. 3-D views of a full annular plate with (a) one-half or (b) two diagonal quadrants of the outer circumferential edge built-in; inner circumferential edges are free for both cases

Using the analysis in Sec. 2, we solved the free vibration problem of a full annular bimorph plate with a free inner circumferential edge and an outer circumferential edge that is built-in with periodicity. PZT-5 [24] was selected as the piezoceramic material for the bimorph plate. For the illustration purpose, two sets of outer circumferential edge conditions were considered: (a) a full annular plate with half of the outer circumferential edge built-in and (b) a plate with two diagonal quadrants of the outer circumferential edge built-in; the other portions are free in both cases. Figure 2 shows the 3-D schematic diagrams of these two cases. We obtained the dispersion relationships using the procedure described in Sec. 2. Fig. 3 shows the dispersion curves for the (a) built-in and (b) free portions of the annular bimorph plate, respectively, with $\overline{r}_0 = 5\pi/3$ and $\hat{\nu} = 0.408$. The effective Poisson's ratio ($\hat{\nu}$) of PZT-5 was used in this illustration. In this figure, the dimensionless frequency $\overline{\kappa\Omega}$ is plotted against $R(\xi)$ and $I(\xi)$, which represent the real and imaginary values of the argument ξ, respectively. Note that a complex branch depicted in Fig. 3 always represents two branches, since its complex conjugate is also a branch. Therefore, whenever the number of branches is mentioned, a complex branch is counted twice. A certain number of these solutions (i.e., dispersion curves) are taken to describe the flexural behavior of the plate sufficiently.

Table 1 gives the natural frequencies calculated for the first five modes of the full annular plate with either set of edge conditions, and Fig. 4 shows the associated mode shapes. A series of computations were performed by using the Maple [25] and the Matlab [26] and the results were compared with those obtained from the ANSYS [27] calculations in Table 3. A total of 19 dispersion branches for the built-in portions and 18 branches for the free portions of the plate (including all the real branches in the frequency range of interest) were included for case (a). Two more branches for each portion were included for case (b) because these were necessary to represent the associated mode shapes properly. The number of branches was determined to maintain an appropriate level of numerical accuracy. The Table shows that the analytical results

are in good agreement with the finite element analysis. The relative error was less than 2 % for most of the cases. However, for the third mode of case (b), the relative error was slightly larger than 2 %, possibly due to the omission of substantial imaginary or complex branches required to represent the associated mode shapes properly. We did not attempt to include any additional branches due to computational limitations, but we believe that the accuracy can readily be improved by including more branches.

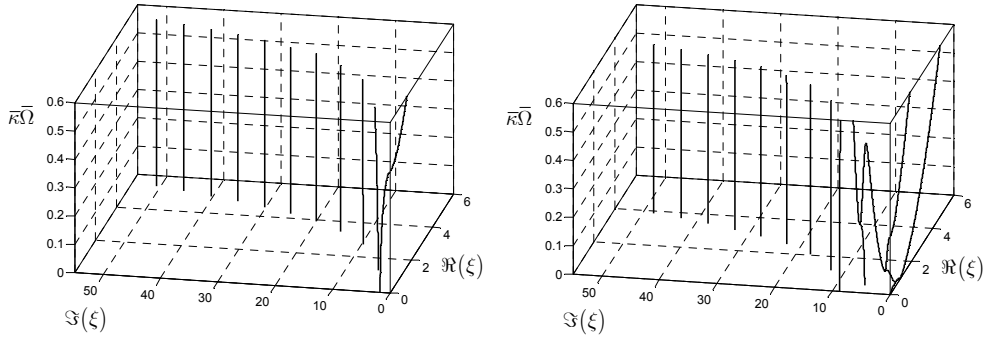

(a) (b)

Fig. 3. Dispersion curves for the (a) built-in and
(b) free outer circumferential portions of the annular bimorph plate

Table 1. Dimensionless natural frequencies (C) for out-of-plane motion of the annular plate with a free inner edge and a periodically built-in outer edge, comparison with a finite element analysis* (F), and relative percent error (e); Case (a): one half of the outer circumferential edge is built-in; Case (b): two diagonal quadrants of the outer circumferential edge are built-in

Mode		1	2	3	4	5
Case (a)	C	0.045285	0.133302	0.258571	0.305640	0.406086
	F	0.045812	0.134650	0.260551	0.319477	0.409701
	e	1.149426	1.001066	0.760156	1.452726	0.882418
Case (b)	C	0.175639	0.176156	0.338366	0.398826	0.448007
	F	0.178366	0.178909	0.346416	0.406566	0.451205
	e	1.528626	1.538809	2.323820	1.903895	0.708816

As expected, the fundamental natural frequency of the plate under periodically built-in outer circumferential edge conditions was much smaller than the natural frequency of the plate under fully built-in edge conditions. The value of this frequency is determined by the spatial frequency of the built-in portions of the plate. Thus, the procedure developed in this study could help in the design of annular bimorph plate sensors and actuators, especially those that require natural frequency adjustments.

Conclusions

Natural frequencies of actuators and sensors composed of polarized piezoceramic bimorph plates must sometimes be adjusted, which can be problematic. To resolve this issue semi-analytically, we first analyzed a more general polar orthorhombic annular sectorial plate with a free inner circumferential edge and a built-in or constrained outer circumferential edge. Using the results of the present study and the dispersion relationships from a previous study [19], we solved the free vibration problem of a full annular bimorph plate with a free inner circumferential edge and an outer circumferential edge that was built in or constrained with periodicity.

Mode	Case (a): (19, 18)*	Case (b): (21, 20)*
1	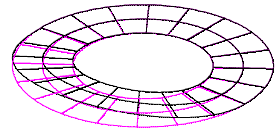	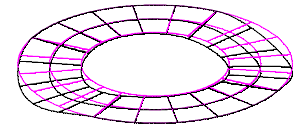
2	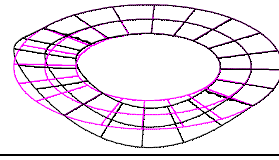	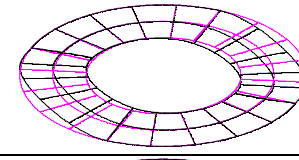
3	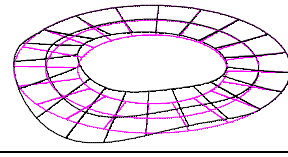	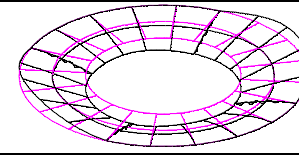
4	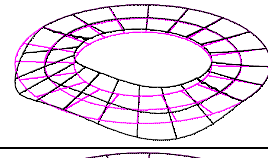	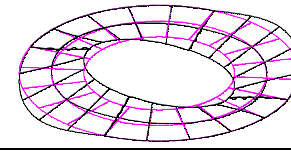
5	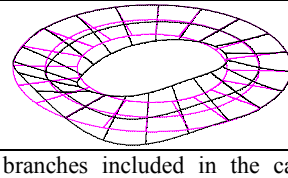	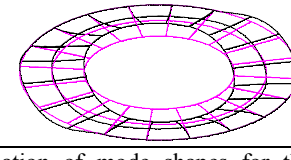

*Number of dispersion branches included in the calculation of mode shapes for the built-in outer circumferential edge portion and the free outer circumferential edge portion.

Fig. 4. First five mode shapes for the flexural motion of the annular plate with free inner edge and periodically built-in outer edge conditions. Case (a): one-half of the outer circumferential edge is built-in; Case (b): two diagonal quadrants of outer circumferential edge are built-in

The variational equation for this plate, which can be pictured as a combination of two types of sectorial plates with an appropriate number of internal edges of discontinuity, was derived using the variational principle. The results obtained in this study were consistent with those of a finite element analysis, which validated the present variational approach. The present analysis demonstrated that the variational approximation method can be applied to treat problems with internal surfaces of discontinuity by introducing the appropriate Lagrange multipliers. Furthermore, it was revealed that the natural frequency varies significantly with the periodicity of the outer edge conditions. We believe that the procedure developed in this study can be used to help design annular bimorph plate sensors and actuators that require natural frequency adjustments. This method can also provide a better understanding of the waves that make up the vibration compared to other methods.

Acknowledgments

This work was supported by the National Research Foundation of Korea (NRF) Grant funded by the Korea Government (MEST) (No. 2012-0005312).

References

[1] Leissa A. W. Vibration of Plates. NASA SP-160, US Government Printing Office, 1969.

[2] **Ramakrishnan R., Kunukkasseril V. X.** Free vibration of annular sector plate. Journal of Sound and Vibration, Vol. 30, Issue 1, 1973, p. 127 – 129.
[3] **Kobayashi H., Nishikawa T., Sonoda K.** Effect of shear deformation on dynamic response of curved slab bridge to moving loads. Proceedings of International Symposium on Geomechanics, Bridges, and Structures, Lanzhou China, 1987, p. 171 – 185.
[4] **Mindlin R. D.** An Introduction to the Mathematical Theory of the Vibration of Elastic Plates. US Army Signal Corps Engineering Laboratory, Fort Monmouth, NJ, 1955.
[5] **Ramaiah G. K., Vijayakumar K.** Natural frequencies of circumferentially truncated sector plates with simply supported straight edges. Journal of Sound and Vibration, Vol. 34, Issue 1, 1974, p. 53 – 61.
[6] **Rubin C.** Vibrating modes for simply supported polar-orthotropic sector plates. Journal of the Acoustical Society of America, Vol. 58, Issue 4, 1975, p. 841 – 185.
[7] **Mukhopadhyay M.** A semi-analytic solution for free vibration of annular sector plates. Journal of Sound and Vibration, Vol. 63, Issue 1, 1979, p. 87 – 95.
[8] **Kim C. S., Dickinson S. M.** On the free, transverse vibration of annular and circular thin sectorial plates subject to certain complicating effects. Journal of Sound and Vibration, Vol. 134, Issue 3, 1989, p. 407 – 421.
[9] **Liew K. M., Kitipornchai S., Xiang Y.** Vibration of annular sector Mindlin plates with internal radial line and circumferential arc supports. Journal of Sound and Vibration, Vol. 183, Issue 3, 1995, p. 401 – 419.
[10] **Yuan J., Dickinson S. M.** On the vibration of annular, circular and sectorial plates with cut-outs or on portionial supports. Computers & Structures, Vol. 58, Issue 6, 1996, p. 1261 – 1264.
[11] **Yang B., Zhou J.** Strip distributed transfer function analysis of circular and sectorial plates. Journal of Sound and Vibration, Vol. 201, Issue 5, 1997, p. 641 – 647.
[12] **Wong W. O., Yam L. H., Li Y. Y., Law L. Y., Chan K. T.** Vibration analysis of annular plates using mode subtraction method. Journal of Sound and Vibration, Vol. 232, Issue 4, 2000, p. 807 – 822.
[13] **Houmat A.** A sector Fourier *p*-element applied to free vibration analysis of sectorial plates. Journal of Sound and Vibration, Vol. 243, Issue 2, 2001, p. 269 – 282.
[14] **Sharma A., Sharda H. B., Nath Y.** Stability and vibration of thick laminated composite sector plates. Journal of Sound and Vibration, Vol. 287, 2005, p. 1 – 23.
[15] **Liang B., Zhang S. F., Chen D. Y.** Natural frequencies of circular annular plates with variable thickness by a new method. International Journal of Pressure Vessels and Piping, Vol. 84, 2007, p. 293 – 297.
[16] **Kukla S., Szewczyk M.** Frequency analysis of annular plates with elastic concentric supports by Green's function method. Journal of Sound and Vibration, Vol. 300, 2007, p. 387 – 393.
[17] **Tiersten H. F.** Linear Piezoelectric Plate Vibrations. Plenum Press, New York, 1969.
[18] **Seok J., Tiersten H. F., Scarton H. A.** Free vibrations of rectangular cantilever plates. Part 1: Out-of-plane motion. Journal of Sound and Vibration, Vol. 271, 2004, p. 131 – 146.
[19] **Seok J., Tiersten H. F.** Free vibrations of annular sector cantilever plates. Part 1: Out-of-plane motion. Journal of Sound and Vibration, Vol. 271, Issue 3-5, 2004, p. 757 – 772.
[20] **Hildebrand F. B.** Advanced Calculus for Applications. Prentice-Hall, Englewood Cliffs, NJ, 1976, Sec. 4.4.
[21] **Morse P. M., Feshback H.** Methods of Theoretical Physics. McGraw-Hill, New York, 1953, Portion I, p. 530 – 531.
[22] **Seok J.** Dispersion relations for cylindrical bending motions of polarized piezoceramic bimorph plates with two facing edges free. International Journal of Solids and Structures, Vol. 42, 2005, p. 1957 – 1981.
[23] **Gutierrez R. H., Laura P. A. A., Felix D., Pistonesi C.** Fundamental frequency of transverse vibration of circular, annular plates of polar orthotropy. Journal of Sound and Vibration, Vol. 230, Issue 5, 2000, p. 1191 – 1195.
[24] **Berlincourt D. A., Curran D. R., Jaffe H.** Piezoelectric and Piezomagnetic Materials. Physical Acoustics, W. P. Mason, New York, 1964.
[25] Maple™, User Manual Release 10.0, Waterloo Maple Inc., 2005.
[26] Matlab™, User Manual Release 7.0.1, Math Works Inc., 2004.
[27] ANSYS Inc., ANSYS Reference Manual Release 10.0, Canonsburg, Pa., 2006.